Measurements of Neglected Double Stars

Brandon Bonifacio, Calla Marchetti, Ryan Caputo, and Kalée Tock

Stanford Online High School
Stanford, California, United States

Abstract: Double stars with a dim, high delta-magnitude companion are difficult to resolve and measure, and are therefore often neglected despite their high abundance in the galaxy. We measured fourteen of these dim, high delta-magnitude doubles, some from the WDS and some discovered by Gaia but never studied before. Although all of our systems' components have similar parallaxes and proper motions, many of the systems have only a few observations other than what is presented here, making them historically neglected. To resolve the systems, we used PixInsight and AstroImageJ to perform image stacking. Using the measurements from Gaia Data Release 2, we present an escape velocity estimate to assess the likelihood of a system being gravitationally bound. A Monte Carlo method was employed to characterize the error associated with this calculation.

Introduction

Red dwarf stars have masses less than 50 percent that of our Sun and surface temperatures in the range 2500-4000K. Despite their small masses, red dwarfs burn through their hydrogen supplies relatively slowly, giving them long lifespans of about 100 billion years. These extended lifespans imply that the population of red dwarfs is relatively large; it is estimated that they make up 70% of stars in the Universe (Kaufman, 2017). Despite their abundance, however, red dwarfs are less commonly observed in double star studies because imaging them can be problematic. For example, red dwarfs are often located in high delta-magnitude systems, making them difficult to separate from the overwhelming brightness of their corresponding primaries. Also, it is not uncommon for red dwarfs to be fainter than 14th magnitude, which necessitates long exposure times. Because red dwarfs are more difficult to measure, many of these systems are either not imaged or have few observations (Wasson, et al., 2020). We searched the Washington Double Star Catalog (WDS) and Gaia Data Release 2 (DR 2) specifically for these red dwarf stars or stars having other noteworthy characteristics, such as being relatively unobserved or neglected systems.

For each of the systems studied here, we assess the likelihood that the system is gravitationally bound by comparing the system escape velocity to the relative velocity of the component stars. However, both escape velocity and relative velocity are approximate because of the many estimates involved (Caputo, 2020). For example, escape velocity depends on mass, which can be computed from luminosity if the star is on the main sequence. However, the formula for the mass luminosity relationship itself is an approximation, depending on the type of star to which it is applied. Also, if a star's luminosity is not directly available in Gaia DR 2, then it must be estimated from its observed magnitude together with its distance, both of which have their own associated errors. Therefore, in order to evaluate the error on both escape velocity and relative velocity, it is useful to sample the input variable distributions using a Monte Carlo technique.

Target Selection

Target selection was based on a number of criteria. First, the coordinates had to be visible to Ryan Caputo on his telescope in Texas in February, at which time the best RA was between 3 and 15 hours. Declination needed to be above -10 degrees. The instruments used, which are described in the next section, required the separation to be greater than 4 arcseconds. If the system delta magnitude was larger than 3, then its separation needed to be correspondingly higher, as a large difference in magnitudes makes stars more difficult to split. Individual magnitudes were limited to 16 or less, for the sake of imaging time.

To find double star systems satisfying all of these criteria, the GDS1.0 tool was used.

*Received *****DATE HERE*******

GDS1.0 is software (Dave Rowe, 2018) which compiles lists of Gaia DR2 double stars with separation less than 10" from the 1.3 billion stars in Gaia DR2, matching these to systems in the WDS where possible (Wasson et. al., 2020). Using this program, users can extract stars that satisfy specific conditions of RA, Dec, primary star magnitude (Comp 1 Mag), delta-magnitude, separation, and Gravitationally Bound Index (GBI). The GBI is a parameter that estimates the likelihood of a physical relationship based on similarity of parallax and proper motion. Further sorting on Gaia parallax and proper motion produced candidates likely to be true binaries.

Even after narrowing down double star systems according to these criteria, an abundance of possible targets remained. Among those, we were particularly interested in stars with temperatures below 4000K, indicating that they are red dwarfs. We also targeted one star with a temperature above 7000K and a relatively dim absolute magnitude, indicating that it is most likely a white dwarf. Some of the stars we selected have parallax greater than 30 milliarcseconds (mas); these are of particular interest since they are in our solar neighborhood.

Instruments Used

A ZWO ASI 1600mm camera attached to a 6-inch classical Cassegrain was used to image all the double star systems for this study. The Cassegrain has a focal ratio of f/12, giving it a relatively high focal length of 1800 mm. Combined with the small 3.4 μm pixels of the ASI 1600mm, the sampling is 0.4" per pixel. This yields excellent resolution on close double stars, allowing seeing-limited measurements to be made.

To overcome the difficulty of imaging high delta mag systems, an Astronomik IR pass 742nm filter was used in observations specified in Table 2. This filter often removes more light from the primary than the secondary, lowering the delta mag of the system and allowing measurements to be made on otherwise impossibly-difficult pairs. Additionally, a guiding system was employed to improve tracking accuracy. This partially corrects periodic error and polar alignment error for very long exposures. With an aperture of only six inches and a slow focal ratio, photons are at a premium, and reaching 15th magnitude stars requires 10 minute exposures with an open filter. Imaging in the infrared has its benefits: namely, the ability to record higher delta mag stars at closer separations. But this comes at a cost: longer exposure times. Not only does less light pass to the camera, but the ASI 1600mm camera is less sensitive at infrared wavelengths. These effects combine to make it difficult to image the already-faint red dwarfs. Through the 742nm IR filter, a magnitude 14.5 star required 20 minute exposures for the particular telescope used.

Targets

The targets systems of this study are shown in Table 1 together with their parallax and proper motion (PM) data from Gaia DR2. Systems that exist in the WDS are listed by discoverer code, while systems that are not in the WDS are identified by their GDS1.0 ID. For each system, a proper motion ratio (rPM) was calculated. The rPM of the stars is a representation of how similarly they move across the celestial sphere, and it is calculated using the equations below. First, the magnitude of the stars' relative motion is calculated by taking the magnitude of the difference vector between the primary and secondary proper motion vectors, as shown in Equation 1.

In Equation 1, pm_{RA1} is the angular velocity of the primary star in right ascension measured in milliarcseconds per year, pmDec1 is the angular velocity of the primary star in declination measured in milliarcseconds

$$pm_{Mag} = \sqrt{(pm_{RA1} - pm_{RA2})^2 + (pm_{Dec1} - pm_{Dec2})^2}$$

Equation 1: Proper motion of stars

per year, and so on for the variables with a 2 subscript for the secondary star.

After this, the rPM of the stars is calculated by dividing the magnitude of the proper motion by the magnitude of the larger proper motion vector. For example, if the primary star has a larger magnitude of proper motion than the secondary star, then the rPM is given by the below equation.

$$rpm = \frac{pm_{Mag}}{\sqrt{pm_{RA1}^2 + pm_{Dec1}^2}}$$

Equation 2: Relative proper motion of stars

If the secondary star's proper motion is larger, then the subscript becomes a 2 instead of a 1 in the denominator of Equation 2. A small rPM value indicates that the difference in component motions is small relative to the component motions themselves. An rPM below 0.2 is the criterion for classifying the stars as having Common Proper Motion, or CPM (Harshaw, 2016). All of the stars in this study are CPM stars. Note that STF 326AB and LDS 883AC are part of a single triple system, although an orbit has not been established for either system.

System	Parallax of Primary (mas)	Parallax of Secondary (mas)	Proper Motion of Primary (mas/year)	Proper Motion of Secondary (mas/year)	rPM
STF 326AB	44.4±.05	44.4±.07	(264.5±.10, -193.4±.07)	(282.0±.14, -166.5±.1)	.098
LDS 883AC	44.4±.05	44.3±.06	(264.5±.10, -193.4±.07)	(276.9±.15, -179.9±.11)	.056
6763049	9.7±.04	9.7±.06	(86.2±.09, -116.6±.05)	(85.1±.1, -117.4±.06)	.010
6814658	12.2±.05	12.3±.04	(-34.2±.03, -9.3±.07)	(-30.9±.03, -9.9±.08)	.095
KPP 837	6.0±.05	5.94±.03	(10.5±.09, -37.2±.05)	(11.1±.06, -38.1±.03	.029
6709693	6.5±.04	6.5±.03	(18.6±.08, -27.5±.07)	(17.3±.05, -27.9±.04)	.040
6765766	11.4±.07	11.3±.03	(-105.5±.10, 3.8±.07)	(-106.6±.06, 3.5±.03)	.011
HDS 597	9.5±.05	9.7±.06	(-6.8±.09, -16.9±.04)	(-7.8±.10, -16.5±.06)	.059
6770204	16.2±.04	16.2±.08	(-93.5±.09, -27.8±.08)	(-96.2±.74, -28.7±.67)	.028
LDS 905	60.2±.08	62.0±.21	(-228.6±.13, -120.0±.09)	(-205.3±.33, -127.6±.19)	.095
6782185	9.2±.04	9.3±.03	(22.4±.04, -4.1±.05)	(22.2±.04, -3.6±.04)	.013
SKF 365	34.1±.03	34.0±.05	(97.7±.06, -57.8±.06)	(98.5±.13, -49.6±.11)	.073
STT 181	6.5±.05	6.5±.06	(-19.0±.10, 4.3±.06)	(-19.1±.07, 6.0±.05)	.085
STI 2051AB	180.4±.59	181.3±.05	(1303.3±2.05, -2043.8±1.23)	(1335.0±.08, -1947.6±.09)	.041

Table 1: Gaia parallax, proper motion, and rPM (ratio of the PM difference vector magnitude to the longer proper motion vector magnitude) of our target systems.

Noteworthy Stars

A few of our targets have noteworthy characteristics. We have selected a few to discuss in detail below.

The first interesting system is STF 326AB and LDS 883AC. These systems have the same primary star, so together they form a triple rather than a double. However, it is not certain whether the tertiary is gravitationally bound. These stars also proved to be complicated to image process due to the large difference in magnitudes and separation between the stars. STF 326AB has a low separation of 4.58″ and a low delta mag of 1.93, while LDS 883AC has a high separation of 43.75″ and a high delta mag of 5.17. Because of this, the three stars can not be seen at the same time in the same image. As shown in Figure 1, if the contrast is increased so that the primary and secondary are distinguishable, the tertiary is so faint that it is barely visible. However, when the contrast is decreased so the tertiary is observable, the primary and secondary seem to have melded together.

Measurements of Neglected Double Stars

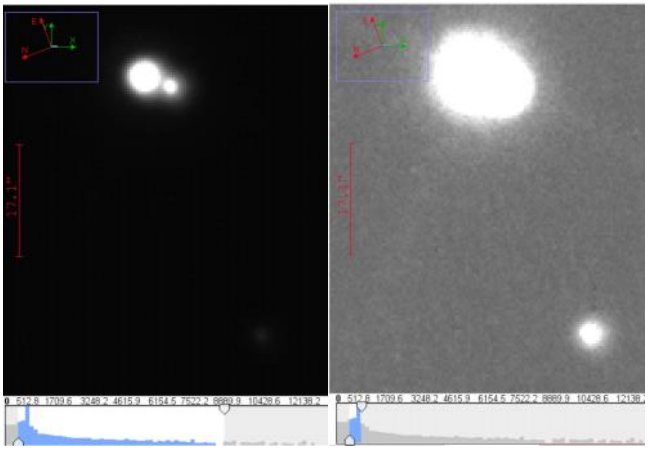

Figure 1: Measuring large delta magnitude systems, with triple in lower right.

The historical measurements of STF 326AB and LDS 883AC were plotted along with the Gaia measurement and our measurement. Figure 2 and Figure 3 are the graphs of the stars' relative positions, which are plotted by fixing the primary's location at the origin. Our measurement for STF 326AB seems to align with the historical trend, but for LDS 883AC there are not enough historical measurements for a trend to be discernible.

Hopmann proposed an orbital solution for this pair in 1967, but it is listed as having incomplete elements (Hopmann, 1967). Hartkopf provided a linear solution in 2017, shown below in Figure 4 (Hartkopf, 2017). The system having both an orbital and linear solution implies that if it is binary, the period is very long.

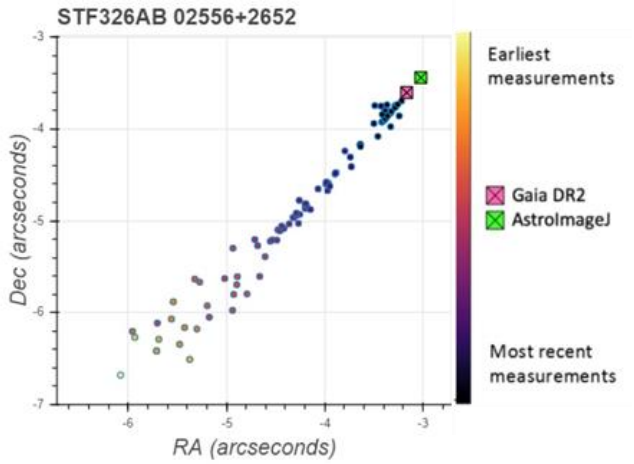

Figure 2: The position of the secondary with respect to the primary

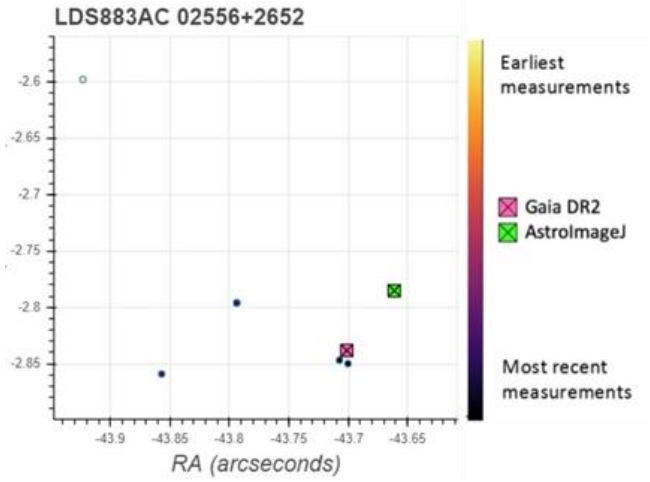

Figure 3: The position of the tertiary with respect to the primary

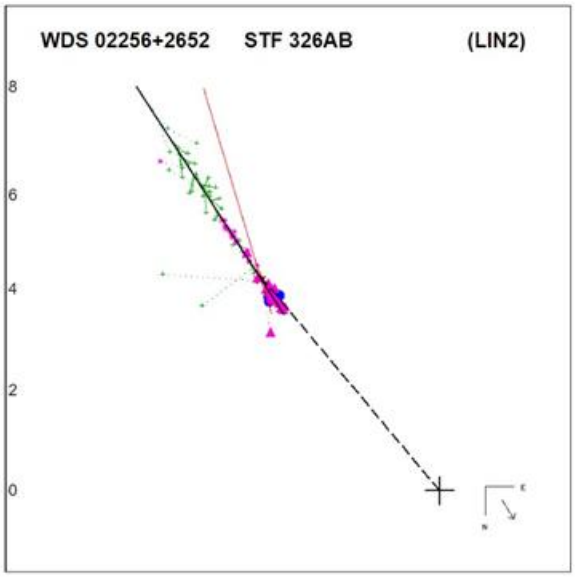

Figure 4: Linear solution for STF 326AB. Note that the orientation is flipped relative to the historical data plot

Another interesting system is STI 2051 AB; this pair is the amalgam of all the characteristics we focused on. Its high parallax of 180 mas puts it the closest to earth of all of our targets, at 5.5 parsec away. The primary and secondary have surface temperatures of 3300K and 7800K, which are the highest and lowest temperatures of any of our targets. The low luminosity of the secondary confirms its status as a white dwarf; type O stars have similar temperatures but much higher luminosities. This makes STI 2051AB a pair with both a red dwarf and a white dwarf. A linear solution was provided by Hartkopf in 2017 (Hartkopf, 2017), and is shown in Figure 5. An updated plot with the Gaia measurement and our measurement is also shown in Figure 6

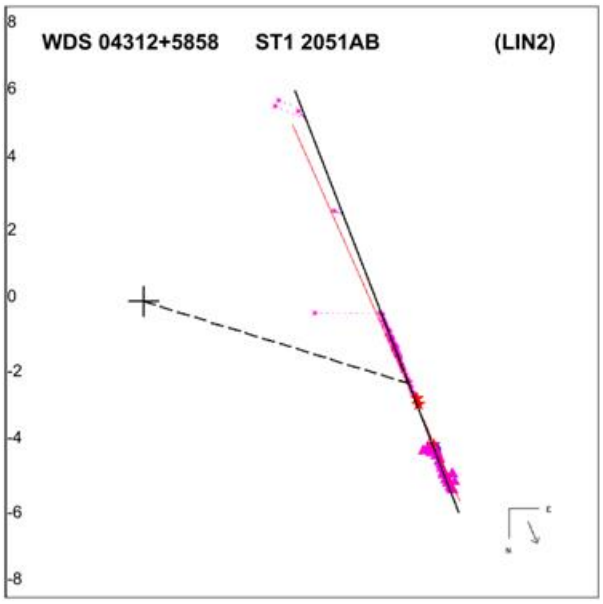

Figure 5: Linear solution for STI 2051AB. Note that the orientation is flipped relative to the historical data plot

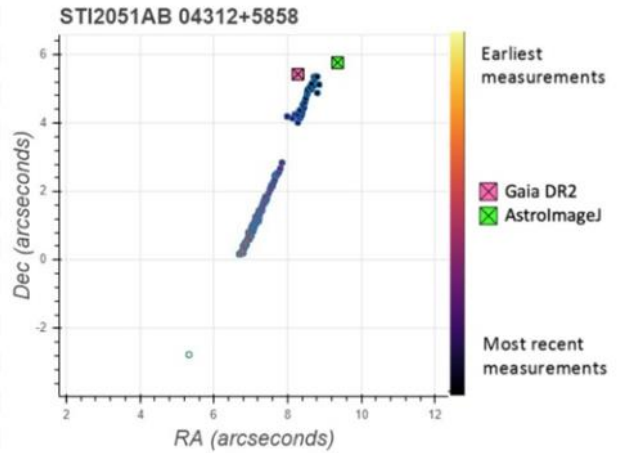

Figure 6: Plot of STI2051 position, with the GAIA measurement and our measurement

Image Stacking

Like LDS883AC, several of these systems have a bright primary and a high delta magnitude, so an exposure time that is optimal for the secondary star would saturate the primary. To increase the signal to noise of the secondary star without increasing exposure time, the images must be stacked. To do this, the images were first aligned relative to a reference frame using the software PixInsight. Then these aligned images were imported into AstroImageJ and stacked into a single image, in which each pixel has the average brightness of the pixels in the component images. Because brightness fluctuations due to noise are random, this has the effect of averaging out the noise without making the stars themselves appear brighter, thereby increasing the signal to noise ratio (SNR). Note that the primary star is not saturated despite it appearing overexposed. The black and white contrast settings are adjusted from their defaults to show the secondary star, and this has the effect of making the brighter primary appear extra bright. However, it is important to note that the pixel values are not saturated in the unstretched image.

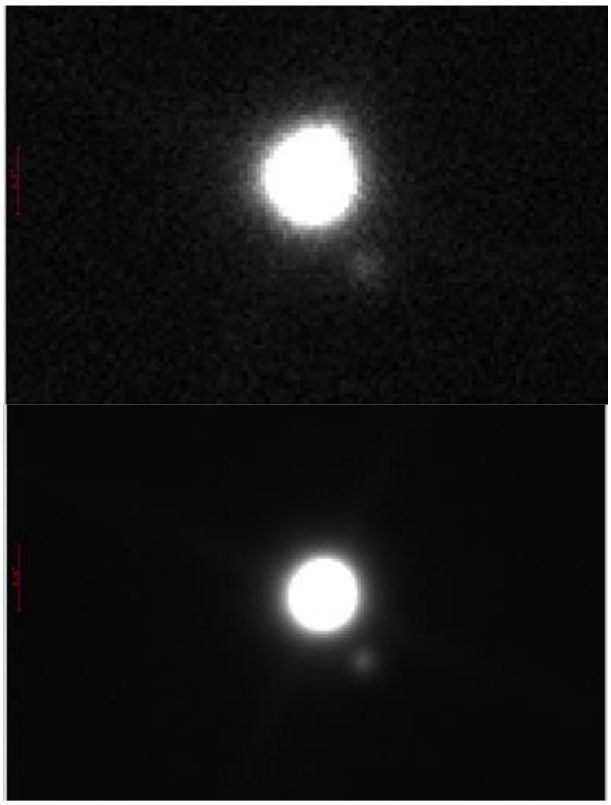

Figure 7: Image of 6814658, of magnitudes 7.3 and 12.3, before stacking (top) and after stacking (bottom) in AIJ.

Rather than stacking all of the files into a single image, multiple stacks were made for each system to create a pseudo-exposure. These pseudo-exposures were then measured and averaged to produce a more accurate overall measurement. Ideally, just enough images are stacked so that the SNR is sufficient for accurate astrometry. If too many images are stacked, then the extra frames are wasted because there is no need for the extra SNR. Images are platesolved in AIJ, and once images are platesolved AIJ automatically calculates PA and separation between two points. Table 2 shows the systems with their delta magnitudes listed, and Figure 7 shows a high delta mag system before and after stacking in AIJ. Table 3 shows how many images were used per stack for each of the systems, as well as the measurements obtained from these stacks.

Measurements of Neglected Double Stars

System	Spectral Type of Primary	Spectral Type of Secondary	Magnitude of Primary	Magnitude of Secondary	Delta Magnitude	Filters Used
STF 326AB	K	K	7.33	9.26	1.93	infrared 742
LDS 883AC	K	G	7.33	12.50	5.17	infrared 742
6763049	K	K	11.91	14.70	2.79	open
6814658	F	K	7.32	12.34	5.02	open
KPP 837	K	K	11.84	13.35	1.52	open
6709693	G	K	11.23	13.53	2.30	infrared 742
6765766	G	K	10.77	13.39	2.62	infrared 742
HDS 597	F	K	8.95	11.96	3.00	infrared 742
6770204	K	M	11.56	13.22	1.65	open
LDS 905	M	M	10.55	12.97	2.42	infrared 742
6782185	F	K	8.36	13.83	5.47	infrared 742
SKF 365	M	M	11.89	14.57	2.68	infrared 742
STT 181	A	G	7.97	11.77	3.80	open
STI 2051AB	M	F	9.70	12.35	2.65	open

Table 2: Spectral types, estimated from Gaia BP-RP and an HR diagram, and magnitudes (in Gaia G) of stars.

System	Date	Number of Images	Images per Stack	Position Angle (°)	Standard Error on Position Angle	Separation (")	Standard Error on Separation
STF 326AB	2020.11	100	20	221.28	.100	4.58	.040
LDS 883AC	2020.11	100	20	266.35	.016	43.75	.011
6763049	2020.11	5	1	130.33	.108	8.95	.018
6814658	2020.11	100	20	257.78	.049	9.89	.017
KPP 837	2020.11	30	7	88.53	.052	7.1	.006
6709693	2020.15	2	1	185.3	.250	8.02	.014
6765766	2020.16	15	1	134.34	.057	7.22	.010
HDS 597	2020.16	21	6	79.82	.057	6.61	.007
6770204	2020.16	10	1	317.56	.048	7.59	.009
LDS 905	2020.16	14	1	348.29	.014	9.98	.002
6782185	2020.16	29	9	356.33	.045	9.23	.006
SKF 365	2020.16	3	1	286.07	.079	8.98	.016
STT 181	2020.16	250	20	262.68	.030	6.75	.002
STI 2051AB	2020.01	10	1	58.60	.024	10.99	.010

Table 3: Measurements of double stars.

Overview of Important Variables

Before the release of Gaia DR2, many optical doubles were incorrectly assumed to be binaries because their component stars appeared relatively close together in the sky and had similar proper motions. However, Gaia DR2 parallax measurements indicated that for some of these systems, the component stars were actually many parsecs apart from each other in the radial direction, making it impossible for them to be gravitationally bound to each other (Dugan et. al, 2019).

Now that Gaia DR2 parallax, PM, and radial velocity measurements are available for many WDS and other systems, we can evaluate the probability that two stars are gravitationally bound together more accurately in terms of the rPM discussed earlier in the paper and three other variables: the three-dimensional distance between the two stars derived below, the system escape velocity derived in Appendix A, and the actual relative velocity of the stars derived later in the paper.

Three-Dimensional Distance

The three-dimensional distance between the stars is the spatial separation between them. This distance alone provides a useful filter because both binary stars would have to be fairly massive and also moving very slowly relative to each other in order to remain gravitationally bound beyond roughly one-tenth of a parsec, so in general, it is unlikely that two stars with a separation of more than one-tenth of a parsec will be gravitationally bound. To be specific, if the two stars each had the mass of our sun, which is unlikely considering the most common star is a red dwarf or a another star that has less mass that our sun, the relative velocity of the stars would have to be less than 400 m/s in order to be gravitationally bound to each other. As can be seen in Table 5, not many star systems have minimum actual velocities less than 400 m/s, so most stars with separations greater than one-tenth of a parsec are not gravitationally bound. Furthermore, most of the stars in this study had a mass less than that of our sun. However, the three-dimensional distance alone can not act as a definite rule for deciding whether stars are bound together because some systems are actually composed of slow, massive stars that can remain coupled at above this distance.

The three-dimensional distance is also used in the expression for the escape velocity of the system. To calculate it, the transverse distance between the stars in parsecs must first be computed using equation 3.

In equation 3, sep is the separation of the stars in arcseconds. This is calculated by AIJ as described above in Image Stacking. The variable p_1 is the parallax of the primary star measured in arcseconds. The choice of the primary star's parallax here is arbitrary, since we are computing the transverse separation only, and the parallaxes of both stars are very similar. Moreover, in the overall calculation of three-dimensional spatial separation for these targets, the transverse separation is usually greatly overshadowed by the radial separation. However, when examining stars with larger differences in parallax, it might be useful to modify this equation to choose the parallax of the star further away from Earth, so that it represents the maximum transverse separation.

$$R_{transverse} = sep * \frac{1^o}{3600''} * \frac{2\pi}{360^o} * \frac{1}{p_1}$$

Equation 3: Transverse separation of stars where p_1 is the parallax of the primary star.

Once the transverse separation has been found, the three-dimensional distance in parsecs between the stars can be computed using equation 4.

$$R = \sqrt{|\frac{1}{p_1} - \frac{1}{p_2}|^2 + R^2_{transverse}}$$

Equation 4: 3D separation between the stars.

Escape Velocity

The escape velocity of the stars is calculated from the property that the total mechanical energy of the binary star system must be zero for the stars to orbit each other. Otherwise, the stars would not be bound. Through the use of this principle, we can calculate the maximum velocity that a star can have in order to be in a physical orbit with another star (Thornton, 2004; Richmond, 2020). The escape velocity equation is given below, and the full derivation of it is left to Appendix A.

$$\mathrm{v_{esc}} = \sqrt{\frac{2GM}{r}}.$$

Equation 5: Escape velocity equation of the binary star system where r is the three-dimensional distance between the stars and M is the total mass of the system, which is equal to the mass of the primary plus the mass of the secondary.

To calculate the total mass used in the escape velocity equation, we use a mass-to-luminosity approximation for main-sequence stars that can be summarized by eqation 6 below (Salaris & Cassisi, 2005; Duric 2004; "The Eddington Limit," 2003).

$$M = \left(\frac{L}{0.23}\right)^{0.434783}, \quad L < 0.033015L_{\odot}$$
$$M = L^{0.25}, \quad 0.033015L_{\odot} < L < 16L_{\odot}$$
$$M = \left(\frac{L}{1.4}\right)^{0.2857}, \quad 16L_{\odot} < L < 1.7x10^{6}L_{\odot}$$
$$M = \left(\frac{L}{3200}\right), \quad 1.7x10^{6}L_{\odot} < L$$

Equation 6: Mass-Luminosity equations where M and L are in units of solar masses and solar luminosities, respectively. As a note, only the first two equations were used in this study due to the nature of the stars we were observing. To use the last equation, truly massive stars would be required.

The luminosity for the stars is determined from Gaia's catalog, but if Gaia does not have the luminosity of the star in its catalog, the following approximation is used from the visual apparent magnitude of the stars using Gaia's filter. First, the absolute magnitude of the star is calculated from equation 7.

$$M_v = m + 5(log(p) + 1)$$

Equation 7: Absolute magnitude of a star estimated from the parallax of the star, p, and the apparent visual magnitude of the star, m.

Once the absolute magnitude is calculated, the luminosity of the star is estimated from Equation 8 below. Then the mass is found from the relation shown in Equation 6, and used in the escape velocity calculation of Equation 5.

$$L = 10^{0.4(4.85-M_v)}$$

Equation 8: Luminosity of the star in solar luminosities.

Relative Velocity

Once the escape velocity for the system has been estimated from Equation 5, it is compared to the relative velocity of the stars to each other. To calculate the actual relative velocity of the system, we first calculate the actual relative transverse velocity, equation 9 below, which is taken by converting the magnitude of the difference in the angular velocity vectors (from Equation 1) from units of mas/yr to kilometers per second. This is done by multiplying by unit conversion factors and the radial distance from the stars to the Earth as shown below. Just like Equation 3, p_1 is taken to be the parallax of the primary star.

This produces the two-dimensional relative velocity, and for some stars, a two-dimensional velocity is the best we can do. However, for the stars for which Gaia has measured radial velocity (RV), we can calculate the

$$v_{transverse} = pm_{Mag} * \frac{1''}{1000mas} * \frac{1^{o}}{3600''} * \frac{2\pi}{360^{o}} * \frac{1}{p_1} * (3.086*10^{13}) \frac{km}{pc} * \frac{1}{3.54*10^{7}} \frac{yr}{s}$$

Equation 9: Transverse velocity of the stars, where pmMag is as found using Equation 1 and p1 is the parallax of the primary star. The choice of the primary's parallax is arbitrary for the same reasoning described earlier.

relative three-dimensional velocity of the stars by taking the square root of the sum of the squares of the two-dimensional relative velocity and the relative RV, as shown in equation 10.

Once this final 3D velocity is computed, it is compared to the escape velocity of the system to determine whether the stars are bound. For example, based on the equations above, KPP 837 has a total mass of roughly 2.8 solar masses (from the mass-luminosity relationship). The distance between its component stars is about 1.25 parsecs. Therefore, the system escape velocity of KPP 837 is roughly 107 m/s. Since the stars are moving at roughly 822 m/s relative to each other in the transverse direction (no radial velocities were available for this star system, so transverse velocity must be used), it would seem unlikely that KPP 837 is a binary. However, based on a complete analysis of this system (which we will conduct below), KPP 837 actually does have a decent probability of being bound. The reason the analysis above seems to contradict this is that it does not fully account for the error on each of the constituent measurements. The errors of the final velocities depend on the errors of each of the inputs in complex ways, and the inputs themselves vary depending on which measurements are available for each star. Because of the complexity inherent in the way the error propagates through these equations, we employ a Monte Carlo series to understand the true likelihood of a binary relationship between the stars.

$$v_{3D} = \sqrt{v_{transverse}^2 + (v_{Rad1} - v_{Rad2})^2}$$

Equation 10: 3D velocity of the stars.

Monte Carlo Analysis

For the stars studied here, the largest sources of error are their parallax values and proper motion vectors. The variation is significant enough to drastically change the resulting analysis. The way that error affects the computation is nontrivial to assess because it affects each star system in a different way. For example, it might skew one system's distribution of escape velocities to the left, but a different system's velocities to the right. If that were not enough, understanding the ways

in which the input distributions themselves are skewed is nontrivial, especially in the case of Gaia parallaxes (Luri et. al, 2018). Therefore, we developed a "catch-all" Monte Carlo method of statistical analysis to understand how error affects the inferences that can be drawn regarding these systems. This Monte Carlo method was roughly based on the curriculum taught by Adam Rengstorf during the Summer Science Program (Rengstorf, 2019).

A Monte Carlo series randomly selects values for the input parameters of separation, parallax, proper motion, radial velocity, and luminosity from their corresponding distributions. Escape velocity and relative velocity are then computed from these values and stored in a large list. After having done this a large number of times, statistical analysis of the list yields a distribution of the resulting velocities that can be used to understand each of their corresponding errors. After a series of tests, one million Monte Carlo iterations seemed to output results that were consistent, so one million is the number of iterations used here.

To provide an example of this so that others may reproduce this method for other star systems, we show the procedure and results of this analysis for KPP 837 below. This is an ideal example due to its relative simplicity and also because it demonstrates the usefulness of this method.

Example Monte Carlo Series

The Monte Carlo series for this research requires twenty-two input parameters for each binary star system. In the case that the radial velocity for both stars is not known, the actual relative velocity calculated is a two-dimensional transverse velocity instead of a three-dimensional velocity. The input parameters for KPP 837 are listed below in Table 4.

The standard error of a value is taken to be equal to the standard deviation of that value's Gaussian distribution. With this interpretation, together with the assumption that the data are normally distributed (in reality, the data are not always normally distributed), one million numbers are selected randomly from the distributions created by each value's range in each system's respective table like the one in Table 4. For each set of values, the calculation is performed for the three-dimensional separation of the stars (Equation 4), the actual relative velocity (Equation 9 or 10), and the escape velocity (Equation 5). The resulting list of these values is ordered, and a 95% confidence interval is created from the center 95% of the data. The example histogram produced for the three-dimensional separation of the components of KPP 837 is shown in Figure 8. As shown, the resulting range of possible three-dimensional distances is skewed right, so the final variable calculated is related to the input variables in complex ways and requires this method of analysis.

The 95% confidence interval produced is where

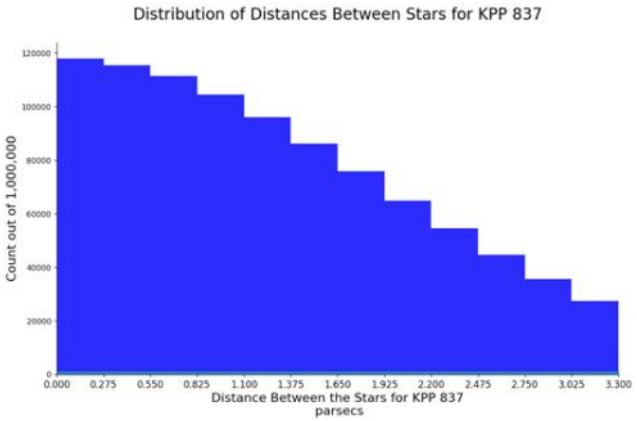

Figure 8: Example Monte Carlo histogram. This histogram was constructed to show how complex relationships exist between the input variables and output variables because, although the input variables were all normally distributed, the output variable is skewed right. Thus, advanced methods are required in order to accurately take the error of the input variables into account. For clarity, the vertical scale is the number of times each range of three-dimensional separations were calculated out of the one million iterations. So, the range of distances between 0 parsecs and 0.275 parsecs occurred roughly 120,000 times, or 12% of the time.

conclusions can be drawn. For this example, the 95% confidence interval for the three-dimensional distance between the stars of KPP 837 is (0.058, 3.979), and this range is retrieved from the summary of all confidence intervals for each star system in Table 5. Since the lower bound of this range is below one-tenth of a parsec, we can be confident that it is entirely possible that these stars are close enough to be gravitationally bound. However, in order to be more sure, the velocities need to be analyzed. The escape velocity and actual velocity ranges for KPP 837 (Table 5) are, respectively, (60, 497) and (720, 930), and the actual velocity is two-dimensional because the radial velocity of the secondary star was not available. Since these two intervals do not overlap at all, we would conclude that it is improbable that these stars are gravitationally boundary. However, since the actual velocity is two-dimensional, it is entirely possible that the stars could be moving towards each other at 223 m/s or more in the radial direction, which would mean that their velocity intervals would overlap. Since 223 m/s is a possible speed with which the stars could be moving towards each other (speeds greater than 500 m/s, while also technically possible, are more unlikely), we can conclude that it is possible that the stars are gravitationally bound. If the velocity

did overlap, we would conclude that it is likely that the stars are gravitationally bound. This method will become more concrete once radial velocities for more stars become known, perhaps in Gaia DR3.

Data Value Name	Data Value	Units
Angular Separation	7.1 ± 0.006	arcseconds
Parallax of Primary	5.9755 ± 0.0463	milliarcseconds
Parallax of Secondary	5.9439 ± 0.0315	milliarcseconds
Primary Right Ascension Proper Motion	10.460 ± 0.092	milliarcseconds/year
Primary Declination Proper Motion	-37.112 ± 0.049	milliarcseconds/year
Secondary Right Ascension Proper Motion	11.058 ± 0.061	milliarcseconds/year
Secondary Declination Proper Motion	-38.110 ± 0.032	milliarcseconds/year
Primary Radial Velocity	4.89 ± 0.31	kilometers/second
Secondary Radial Velocity	Unknown ± Unknown	kilometers/second
Primary Luminosity Range	(0.421, 0.430)	solar luminosities
Secondary Luminosity Range	(0.125, 0.128)	solar luminosities

Table 4: Values for KPP 837 Monte Carlo. Since the second radial velocity is not known, the Monte Carlo will only calculate the actual transverse velocity and use that for the two-dimensional velocity.

Results

Table 5 shows the confidence interval results of the Monte Carlo code for each star system.

Based on the results of the Monte Carlo, we can determine quite a bit about the characteristics of the star system we are studying. Take star system LDS 883 AC, for example. Having a minimum three-dimensional separation of less than one-tenth of a parsec is a good sign that they could be gravitationally bound to each other as shown in the table above. None of the stars with a minimum three-dimensional separation greater than 0.1 parsecs have overlapping relative and escape velocities, and the same can be said for many of the systems with minimum separations slightly smaller than 0.1 parsecs. In LDS 883 AC's 3D separation confidence interval, the minimum separation between the stars is about 0.011 parsecs. Therefore, LDS 883 AC's component stars could be close enough to form a physical binary star system. Furthermore, the confidence intervals for LDS 88C's escape velocity and actual velocity significantly overlap with a common range of 542 m/s. Taking this into account, we can consider it likely that LDS 883 AC is a binary star system.

On the other hand, consider HDS 597. The minimum 3D separation of the component stars is 1.448 parsecs. This is an extremely large distance between the stars, so the results of this analysis would not support a conclusion that HDS 597 is gravitationally bound. Furthermore, the confidence intervals for the escape and relative velocities are not close to overlapping, so based on this data analysis we should be skeptical of an orbital solution for HDS 597 if this star system has not been observed for a long time or if a linear model for the motion of the stars works just as well as an elliptical model for the motion.

Based on the data generated by the Monte Carlo analysis, the binary star systems can be classified into three groups: probable, possible, and improbable to be physically bounded. The probable group consists of stars whose separation confidence interval includes values near (perhaps 0.15 parsecs, for example, if the system consists of massive stars) or below one-tenth of a parsec and whose escape and relative velocity intervals overlap. Possible systems are systems where the confidence intervals are almost fulfilling the requirements for a likely system in a way that the radial velocity not accounted for could explain the difference between the intervals, and an improbable system's confidence intervals are not close to fulfilling these requirements. These groupings are shown in Table 6.

When drawing conclusions from this data, it is best to keep in mind that even a slight error in the data collection of the parallax angle could skew the results drawn for a star, so researchers should not place too much weight on the values of this table until

System	95% Confidence Interval for 3D Separation (Parsecs)	95% Confidence Interval for Escape Velocity (m/s)	95% Confidence Interval for Actual Relative Velocity (m/s)	Type of Actual Relative Velocity
STF 326 AB	(0.00138, 0.0901)	(402, 3266)	(3035, 3087)	2D
LDS 883 AC	(0.0113, 0.785)	(110, 923)	(381, 1122)	2D
6763049	(0.0288, 1.917)	(71, 577)	(532, 727)	2D
6814658	(0.084, 1.611)	(116, 504)	(1137, 1198)	2D
KPP 837	(0.058, 3.979)	(60, 497)	(720, 930)	2D
6709693	(0.068, 3.672)	(64, 470)	(744, 978)	2D
6765766	(0.0703, 2.012)	(84, 452)	(317, 487)	2D
HDS 597	(1.45, 4.779)	(63, 114)	(486, 4338)	3D
6770204	(0.0113, 0.787)	(110, 922)	(381, 1124)	2D
LDS 905	(0.362, 0.596)	(90, 115)	(1673, 1767)	2D
6782185	(0.0283, 1.734)	(105, 829)	(188, 302)	2D
SKF 365	(0.0168, 0.208)	(148, 524)	(991, 1051)	2D
STT 181	(0.0569, 4.066)	(82, 695)	(1002, 1188)	2D
STI 2051AB	(0.00166, 0.0620)	(203,1241)	(2313, 2435)	2D

Table 5: Monte Carlo results for the 3D separation, escape velocity, actual relative velocity, and actual relative velocity type for the systems of stars studied in this research. The values in each range are the minimum and maximum values for each confidence interval.

Probably Gravitationally Bound	Possibly Gravitationally Bound	Improbably Gravitationally Bound
STF 326 AB	STI 2051AB	HDS 597
LDS 883 AC	6814658	LDS 905
6763049	KPP 837	
6765766	6709693	
6770204	SKF 365	
6782185	STT 181	

Table 6: Binary Star Systems categorized as probably, possibly, or improbably gravitational bounded.

scientists have developed excellent methods for measuring the parallaxes of stars with less error and more consistency. The mass-luminosity relationships might also miscalculate the mass of the stars since the equations are estimations. Furthermore, most of the actual velocities for these stars were 2D velocities because many of the systems lacked radial velocity measurements in Gaia. Hopefully there will be more radial velocity measurements in future Gaia catalogs.

Conclusion

These methods provide a means of observing double star systems that previously have been difficult to measure, such as red dwarf binaries. By using filters and stacking images in AstroImageJ, angular separation and position angle can be measured for these stars. Furthermore, a Monte Carlo method of error analysis can be used to estimate the likelihood that the component stars of a double star system are gravitationally bound to each other. This technique involves calculating confidence intervals for the separation between the stars, the escape velocity for the system, and the actual relative velocity of the stars. However, because slight

deviations in parallax and proper motion can have profound effects on the results of these methods, the technique outlined here can be expected to improve corresponding to the precision of the data available in future Gaia data releases.

Acknowledgements

Rick Wasson graciously gifted the Astronomik IR pass 742nm filter, along with several other filters and a filter wheel. These were integral to the success of this project.

This research was made possible by the Washington Double Star catalog maintained by the U.S. Naval Observatory, the Stelledoppie catalog maintained by Gianluca Sordiglioni, Astrometry.net, and AstroImageJ software which was written by Karen Collins and John Kielkopf. This work has also made use of data from the European Space Agency (ESA) mission Gaia (https:// www.cosmos.esa.int/gaia), processed by the Gaia Data Processing and Analysis Consortium (DPAC, https:// www.cosmos.esa.int/web/gaia/dpac/ consortium). Funding for the DPAC has been provided by national institutions, in particular the institutions participating in the Gaia Multilateral Agreement.

References

Rengstorf, A. Lecture Notes on Orbital Determination. New Mexico Institute of Mining and Technology, July 2019.

Caputo, R., Bonifacio, B., Datar, S., Dehnadi, S., Lian E, Green, T., Koodli, K., Koubaa, E., Marchetti, C., Nair, S., Olson, G., Perian, Q., Singh, G., Wang, C., Yeung, P., Robertson, P., Chalcraft, E., Tock, K., 2020. "Observation and Investigation of 14 Wide Common Proper Motion Doubles in the Washington Double Star Catalogue", *Journal of Double Star Observations*, 16 (2), 173-182.

Dugan, O., Robinson, T., Carmeci, F., Tock, K., 2019. "CCD Measurements and Reclassification of WDS 07106 +1543 to an Optical Double", *Journal of Double Star Observations*, 15 (1), 119-129

Duric, Nebojsa (2004). Advanced astrophysics. Cambridge University Press. p. 19. ISBN 978-0-521-52571-8.

Harshaw, Richard, 2016, "CCD Measurements of 141 Proper Motion Stars: The Autumn 2015 Observing Program at the Brilliant Sky Observatory, Part 3", *Journal of Double Star Observations*, 12 (4), 394-399.

Hopmann, J., 1967. "Untersuchungen an zwolf visuellen Dopplesternen" ("Studies of Twelve Visual Double Stars"). Mitt. Univ. Sternw. Wien, Vol. 13, 49 - 88.

Hartkopf, W.I. and Mason, B.D. "Catalog of Rectiline ar Elements", v 2017.09.20.

Kaufman, M., 2017 "Red Dwarf Stars and the Planets Around Them"

Luri, X., A. G. A. Brown, L. M. Sarro, F. Arenou, C. A. L. Bailer-Jones, A. Castro-Ginard, J. de Bruijne, T. Prusti, C. Babusiaux,, and H. E. Delgado, 2018. "Gaia Data Release 2: Using Gaia parallaxes" Astronomy and Astrophysics, 616, A9, 1 - 19.

Richmond, M. (n.d.). The "Reduced Mass" approach. Retrieved March 8, 2020, from http://spiff.rit.edu/classes/phys440/lectures/reduced/reduced.html

Rowe, D., 2018. Gaia (DR2)Search Program. Private Communication.

Salaris, Maurizio; Santi Cassisi (2005). Evolution of stars and stellar populations. John Wiley & Sons. pp. 138–140. ISBN 978-0-470-09220-0.

"The Eddington Limit (Lecture 18)" (PDF). jila.colorado.edu. 2003. Retrieved 2020-02-21

Thornton, S., Marion, B., 2004 Classical Dynamics of Particles and Systems. Cengage Learning, Fifth edition, Chapter 8.

Wasson, R., Rowe, D., Russell, G., 2020 "Observation of Gaia (DR2) "New" Red or White Dwarf Binary Stars in the Solar Neighborhood", *Journal of Double Star Observations*, 16 (3), 208-228.

Hopmann, J, 1967. Untersuchungen an zwolf visuellen Dopplesternen, Mitteilungen der Universitaets-Sternwarte Wien, Vol. 13, pp 49-88.

APPENDIX A
Derivation of Escape Velocity Equation

First we represent the position of both stars as vectors in Cartesian coordinates with our Sun at the origin. This is shown in Figure 1 below, where CM is the center of mass of the system, R is the position vector between the Earth and the center of mass, and r, as the difference between r_1 and r_2: $r = r_1 - r_2$.

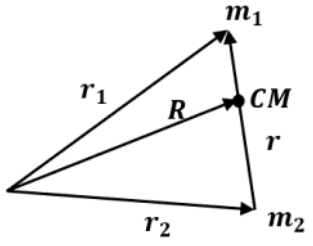

Figure 1: The primary star has a position r1 and a mass m1, and the secondary star has a position r2 and a mass m2 relative to the origin of the coordinate system.

Measurements of Neglected Double Stars

If we put the center of mass of the system as the origin of the coordinate system, the positions of the stars can be redefined for simpler calculations as in Figure 2.

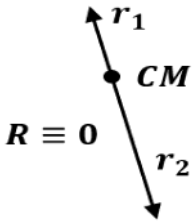

Figure 2: Primary and secondary stars relative to the center of mass of the double star system.

From the inertial reference frame of the center of mass, the following relations must hold:

$$m_1\vec{r_1} + m_2\vec{r_2} = 0$$

Equation 1: Definition of center of mass.

$$\vec{r_1} = \frac{m_2}{m_1+m_2}\vec{r}$$

Equation 2

$$\vec{r_2} = \frac{-m_1}{m_1+m_2}\vec{r}$$

Equation 3

The total kinetic energy of this system is the sum of the kinetic energies of the individual stars as measured from the inertial center of mass reference frame, expressed in Equation 4.

$$T = \frac{1}{2}m_1\dot{r_1}^2 + \frac{1}{2}m_2\dot{r_2}^2$$

Equation 4 : Total kinetic energy for this system where the magnitudes of vectors are shown without arrows and time derivatives are designated by dots.

Plugging the relations of Equations 2 and 3 into Equation 4, we obtain the result shown in Equation 5.

$$T = \frac{1}{2}(m_1\frac{m_2^2}{(m_1+m_2)^2}\dot{r}^2 + m_2\frac{m_2^2}{(m_1+m_2)^2}\dot{r}^2) = \frac{1}{2}\frac{m_1m_2}{m_1+m_2}\dot{r}^2$$

Equation 5: Total kinetic energy for this system in terms of the relative velocities of the stars.

Since the total energy of the system is zero, the potential energy U is equal to the inverse of the kinetic energy in Equation 5. To find an expression for U, we take the primary star as a single particle in free space. This particle is not bound by any system, so its gravitational potential energy is zero. When a new particle (the secondary star) is brought from a faraway distance to a position near the primary, the gravitational potential energy decreases because of the attraction of the two masses to each other. The magnitude of the decrease is equal to the gravitational force integrated over the distance separating the two stars as they are brought into proximity, as shown in Equation 6.

$$\mathrm{U} = \int_r^\infty \frac{-Gm_1m_2}{r^2}dr = \frac{-Gm_1m_2}{r}$$

Equation 6: The potential energy of a star system whose secondary star, of mass m_2, is brought from a faraway distance into a position close to the primary star, of mass m_1.

Finding the escape velocity of this system involves calculating the relative velocity of the stars subject to the constraint that the system has a total energy of zero. The derivation is shown below.

$$\frac{1}{2}\frac{m_1m_2}{m_1+m_2}v^2 = \frac{Gm_1m_2}{r}$$

Equation 7: The kinetic energy of the system is equal to the positive value of the potential energy

$$v = \sqrt{\frac{2G(m_1+m_2)}{r}} = \sqrt{\frac{2GM}{r}}$$

Equation 8: The escape velocity of the star system, where M = m1 + m2 is the total mass of the system.